Supplementary Information for "Coherent oscillation between phonons and magnons"

Tomosato Hioki,[1,2,*] Yusuke Hashimoto,[1] and Eiji Saitoh[1,2,3]

[1] *Advanced Institute for Materials Research, Tohoku University, Sendai 980-8577, Japan*
[2] *Department of Applied Physics, Faculty of Engineering, University of Tokyo, Tokyo 113-8656, Japan*
[3] *Institute for AI and Beyond, The University of Tokyo, Tokyo 113-8656, Japan*

(Dated: April 8, 2022)

I. SUPPLEMENTARY NOTE1: MATERIAL CHARACTERIZATION

In this note, we experimentally characterize the magnetic property of the sample used for the main experiment. We used the $Lu_2Bi_1Fe_{3.4}Ga_{1.6}O_{12}$ (LuIG) film with the thickness of 1.8 µm grown on [001] plane of GGG substrate. The magnetic anisotropy constant of the sample was evaluated by angular dependence of the ferromagnetic resonance field. In Supplementary Figure 1(a), we show the angular dependence of the ferromagnetic resonance (FMR) spectra measured using a microwave cavity. We observed the shift of spectrum peaks as a function of the relative angle between the crystallographic axis and external magnetic field with the period of 90°. Supplementary Figure 1(b) shows the angular dependence of the peak field extracted from the FMR spectra shown in Supplementary Figure 1(a). The angular dependence exhibits clear sinusoidal angular dependence owing to the cubic anisotropy. We fit the data with the formula for the FMR field as follows,

$$H = \frac{1}{2}\left[-(\alpha+\beta+4\pi M_\mathrm{s}) + \sqrt{(\alpha+4\pi M_\mathrm{s}-\beta)^2+4\omega^2/\gamma^2}\right], \tag{1}$$

$$\alpha = \frac{2K_\mathrm{c}}{M_\mathrm{s}}\cos 4\theta, \tag{2}$$

$$\beta = -\frac{2K_\mathrm{u}}{M_\mathrm{s}} + \frac{K_\mathrm{c}}{2M_\mathrm{s}}\left(3+\cos 4\theta\right), \tag{3}$$

where $\gamma = 2\pi \times 2.8 \times 10^{10}$ $[\mathrm{Hz}\cdot\mathrm{T}^{-1}]$ is the gyromagnetic ratio, $\omega = 2\pi \times 9.44 \times 10^9$ [Hz] is the measured frequency, K_u is the uniaxial anisotropy constant, K_c is the cubic anisotropy constant, M_s is the saturation magnetization. By fitting the experimentally obtained data, we could estimate the anisotropy of the material to be $K_\mathrm{c} = 73.0$ $[\mathrm{J}\cdot\mathrm{m}^{-3}]$,

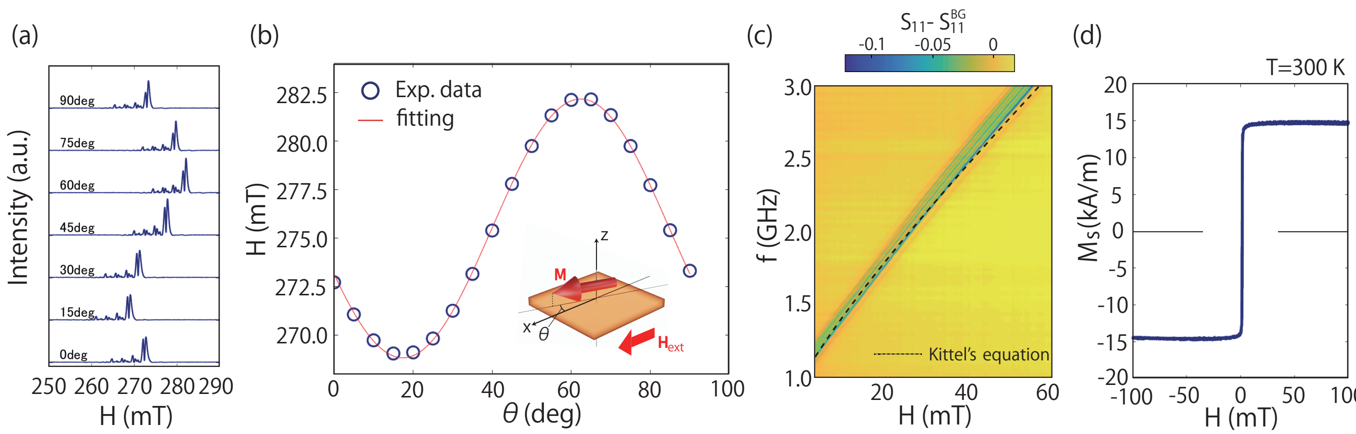

Supplementary Figure 1. Integrated spectrum of ferromagnetic resonance at different in-plane angles. (b). Experimental data of the FMR magnetic field and fitting of the data. The relative angle θ is defined as the angle between crystallographic axis **x** and external magnetic field as shown in the inset. (c). An absorption spectrum of the sample and Kittel's equation calculated from the parameter of LuIG. (d) M-H curve measured by VSM at T=300 K.

* tomosato.hioki.d7@tohoku.ac.jp

$K_\mathrm{u} = -767.5$ [$\mathrm{J \cdot m^{-3}}$]. The calculated resonance field is consistent with the experimentally obtained resonance fields, which is confirmed in Supplementary Figures 1(b) and (c). We plotted Kittel's equation, a relation between ferromagnetic resonance frequency and magnetic field as follows

$$\omega = \gamma\sqrt{H_\beta\left(H_\alpha + 4\pi M_\mathrm{s}\right)}, \tag{4}$$

where H_α and H_β are the anisotropic effective magnetic field defined as follows,

$$H_\alpha = H_0 + \alpha = H_0 + \frac{2K_\mathrm{c}}{M_\mathrm{s}}\cos 4\theta, \tag{5}$$

$$H_\beta = H_0 + \beta = H_0 - \frac{2K_\mathrm{u}}{M_\mathrm{s}} + \frac{K_\mathrm{c}}{2M_\mathrm{s}}(3 + \cos 4\theta). \tag{6}$$

The saturation magnetization of the material is independently measured by Vibrating Sample Magnetometer (VSM) as M_s=14.8 [$\mathrm{kA \cdot m^{-1}}$] as shown in Supplementary Figure 1(d). The Gilbert damping of the Kittel mode is evaluated by using ferromagnetic resonance measurement, of which value is $\alpha_\mathrm{G} = 2.2 \times 10^{-4}$.

II. SUPPLEMENTARY NOTE2: OPTICAL SETUP FOR TIME-RESOLVED MAGNETO-OPTICAL IMAGING

In this note, we explain the technical detail of time-resolved magneto-optical imaging. Supplementary Figure 2(a) shows the schematic illustration of the optical setup for time-resolved magneto-optical imaging.

We switched on and off the pump pulse with a mechanical shutter to measure the magneto-optical images with and without the spin-wave excitation by the pump pulse. A variable ND filter controls the power of the pump pulse, and a metallic slit controls the shape of the pump pulse focus. The prepared pump pulse is guided to the sample with a pulse splitter and objective lens from the opposite orientation to the probe pulse so that the transmitted pump pulse does not travel into the CCD camera. The probe pulse is linearly polarized along the y-axis using a half-waveplate and polarizer and guided to the sample with a lens.

Supplementary Figure 3 shows a schematic illustration of the optical setup to realize measurement of the polarization angle of the probe pulse [1]. Faraday rotation at each point is obtained by measuring the change of the transmitted light's intensity as a function of the angle of the half-waveplate mounted before an analyzer. When the polarization of the light rotates by θ_F, and the light acquires the Faraday rotation of θ_F, the polarization of the transmitted light is described by Jone's matrices setting the matrices as Supplementary Figures 3. The intensity of the electric field is written as follows,

$$\begin{aligned}\mathbf{E} = &\begin{pmatrix} 1 & 0 \\ 0 & 0 \end{pmatrix}\begin{pmatrix} \cos(\frac{\pi}{2}+\theta) & -\sin(\frac{\pi}{2}+\theta) \\ \sin(\frac{\pi}{2}+\theta) & \cos(\frac{\pi}{2}+\theta) \end{pmatrix} \\ &\cdot \begin{pmatrix} e^{i\pi/2} & 0 \\ 0 & e^{-i\pi/2} \end{pmatrix}\begin{pmatrix} \cos(-\frac{\pi}{2}-\theta) & -\sin(-\frac{\pi}{2}-\theta) \\ \sin(-\frac{\pi}{2}-\theta) & -\cos(-\frac{\pi}{2}-\theta) \end{pmatrix} \\ &\cdot \begin{pmatrix} \cos\theta_\mathrm{F} + i\eta_\mathrm{F}\sin\theta_\mathrm{F} & -\sin\theta_\mathrm{F} + i\eta_\mathrm{F}\cos\theta_\mathrm{F} \\ \sin\theta_\mathrm{F} - i\eta_\mathrm{F}\cos\theta_\mathrm{F} & \cos\theta_\mathrm{F} + i\eta_\mathrm{F}\sin\theta_\mathrm{F} \end{pmatrix}\begin{pmatrix} 0 \\ 1 \end{pmatrix},\end{aligned} \tag{7}$$

where, the two component of the $\mathbf{E}$ corresponds to E_x and E_y, θ is a rotation angle of the $\lambda/2$ plate. Due to the initial polarization of the incoming light, only the y component becomes non-zero. The intensity of the electric field of the transmitted light is written as follows,

$$x = \cos 2\theta\left(\mathrm{i}\sin\theta_\mathrm{F} + \eta_\mathrm{F}\cos\theta_\mathrm{F}\right) - \sin 2\theta\left(\mathrm{i}\cos\theta_\mathrm{F} - \eta_\mathrm{F}\sin\theta_\mathrm{F}\right). \tag{8}$$

The intensity of the light is given by the square of the intensity of the electric field, written as follows,

$$|x|^2 = \sin^2\left(2\theta - \theta_\mathrm{F}\right) + \eta_\mathrm{F}^2\cos^2(2\theta - \theta_\mathrm{F}) \tag{9}$$

$$\simeq 8\left(\theta - \frac{\theta_\mathrm{F}}{2}\right)^2\left(1 - \eta_\mathrm{F}^2\right) + \eta_\mathrm{F}^2. \tag{10}$$

We analyzed the images taken at different θ to fit the θ-dependence of the intensity $|x|^2$ in a pixel-wise manner. By fitting the obtained data with Eq. 10, we can obtain the Faraday rotation θ_F, which gives us the Faraday rotation image. Supplementary Figure 2(b) shows the laser intensity image 3.5 ns after the pump pulse irradiation. The pump pulse is focused on a vertical line so that the magnons with wavevector parallel to the horizontal axis are excited,

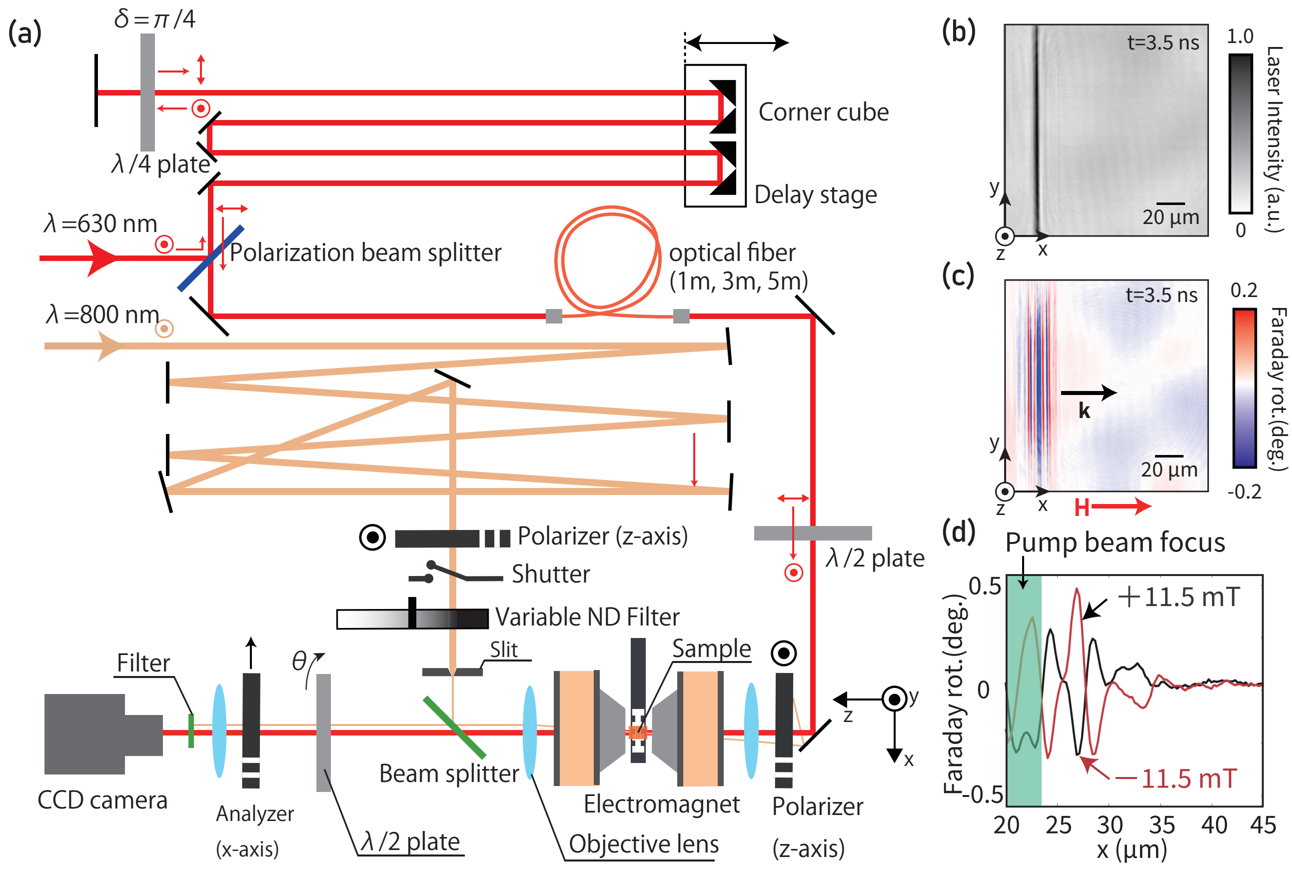

Supplementary Figure 2. (a). A schematic of the configuration of the optical components for Time-resolved magneto-optical imaging. (b). Laser intensity image obtained 3.5 ns after the pump pulse laser irradiation. Black arrow indicates propagation orientation of the observed waves (c). Faraday rotation image obtained 3.5 ns after irradiation. (d). Spatial dependence of Faraday rotation. Green filled area represents where the pump pulse laser is focused on.

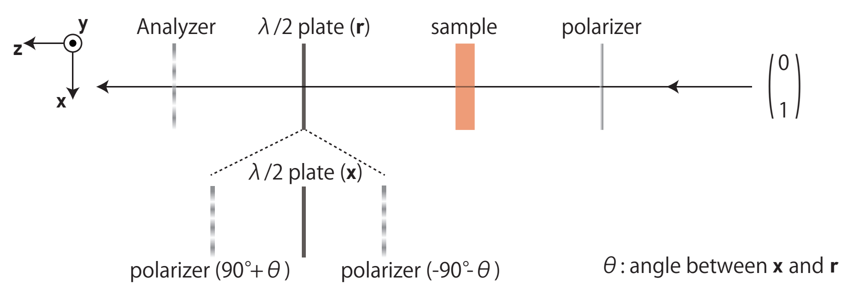

Supplementary Figure 3. A schematic of optical components for the magneto-optical imaging. Here we suppose light with perfectly polarized to y-axis enters to the setup as shown in the right end of the figure.

as shown in Supplementary Figure 2(c). In Supplementary Figure 2(d), we show the magnetic field dependence of the polarization change due to the pump pulse irradiation. The sign of the signal becomes opposite by inverting the external magnetic field, demonstrating that the polarization change is mainly due to the magneto-optical Faraday rotation.

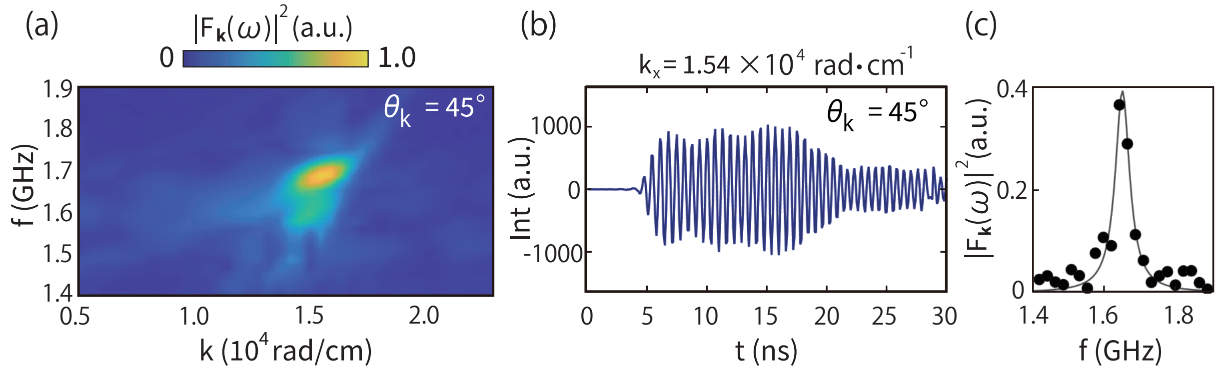

Supplementary Figure 4. (a) Power spectrum $|F_{\mathbf{k}}(\omega)|^2$ under $\theta_{\mathbf{k}} = 45°$ condition. (b) Magnon amplitude $F_{\mathbf{k}}(t)$ at $k_x = 1.55 \times 10^4 \mathrm{rad} \cdot \mathrm{cm}^{-1}$. (c) Power spectrum plot $|F_{\mathbf{k}}(\omega)|^2$ at $k_x = 1.55 \times 10^4$ rad $\cdot$ cm^{-1}. Errors of the data are evaluated as a standard deviation, which is smaller than the data plot.

III. SUPPLEMENTARY NOTE3: MAGNETO-OPTICAL MEASUREMENT UNDER $\theta_{\mathbf{k}} = 45°$ CONDITION

In this note, we show the experimental result obtained under $\theta_{\mathbf{k}} = 45°$ condition, where the coupling between longitudinal (LA) phonons and magnons is maximized. We turn the slit angle to 45° so that we could excite magnon-polaron with the wavevector forming $\theta_{\mathbf{k}} = 45°$ with respect to external magnetic field. In Supplementary Figure 4(a), we show the wavenumber-frequency spectrum of $|F_{\mathbf{k}}(\omega)|$. The single spectral peak appears at $k_x = 1.55 \times 10^4$ rad$\cdot$cm^{-1}. Supplementary Figure 4(b) shows the $\tilde{F}_{\mathbf{k}}(t)$ at the spectral peak wavenumber. The temporal signal appears at $t = 5$ ns and monotonically decreases as time pasts without exhibiting oscillation. Supplementary Figure 4(c) shows the power spectrum obtained from the data plotted on the Supplementary Figure 4(b), which exhibits a single peak. Therefore, the coherent oscillation between magnons and LA phonons are not observed in our experimental setup. This may be owing to the large dissipation of magnon mode at $\theta_{\mathbf{k}} = 45°$, however the detail discussion of the disappearance of coherent oscillation under the $\theta_{\mathbf{k}} = 45°$ is beyond our scope.

SUPPLEMENTARY REFERENCES

[1] Y. Hashimoto et al., Ultrafast time-resolved magneto-optical imaging of all-optical switching in GdFeCo with femtosecond time-resolution and a μm spatial-resolution, Rev. of Sci. Instr. **85**, 063702 (2014).